

Strained $\text{Si}_{1-x}\text{Ge}_x$ Alloys for Silicon-based Heterojunction Bipolar Transistors

J.C. Sturm, E.J. Prinz, P.V. Schwartz, and Z. Matutinovic-Krstelj
 Department of Electrical Engineering
 Princeton University
 Princeton, NJ 08544

Introduction

Bipolar transistors traditionally have been used for the fastest forms of silicon integrated circuitry, such as the emitter coupled logic (ECL) gate configuration. Silicon bipolar transistors, however, suffer from an inherent emitter efficiency/base resistance trade-off which imposes limits on how far those devices may be scaled. The advent of the strained $\text{Si}_{1-x}\text{Ge}_x$ alloy material system has made it possible to bypass these traditional scaling limits by enabling the development of narrow-bandgap-base $\text{Si}/\text{Si}_{1-x}\text{Ge}_x/\text{Si}$ heterojunction bipolar transistors (HBT's). This paper will describe the basic properties of $\text{Si}_{1-x}\text{Ge}_x$ strained layers, how HBT's alleviate the current gain/base resistance trade-off, and what impact they can have on digital and analog silicon-based integrated circuits.

Fundamentals of $\text{Si}_{1-x}\text{Ge}_x$ and HBT's

Two desirable properties of bipolar transistors are a high current gain (I_C/I_B) and a low base resistance. Since the collector current I_C and hence the emitter efficiency are inversely proportional to base doping, high current gains require a low base doping in homojunction transistors. However, virtually all other properties of the transistor desirable for submicron scaling and high current densities require heavy base doping. These properties include a low base resistance for fast circuit operation, a reduction of high level injection effects, and the elimination of punchthrough for thin base widths.

This emitter efficiency/base resistance trade-off can be overcome by making the emitter and base out of semiconductors with different bandgaps. For example, lowering the bandgap in the base presents a smaller barrier to electrons in the emitter compared to a homojunction device at the same bias condition with similar dopings (Fig. 1). This will lead to a larger electron current from emitter to collector (I_C). Since the barrier for holes from the base to emitter in the two devices is similar, the hole currents which comprise I_B should be similar. Therefore the current gain (I_C/I_B) will be much larger in the HBT than in a homojunction device with similar doping. The high current gain, however, can be traded off for a reduced base resistance by increasing the base doping. In this way, the basic emitter efficiency/base resistance trade-off in homojunction transistors can be alleviated.

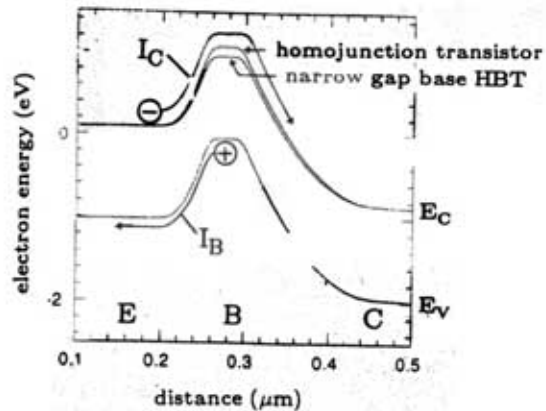


Fig. 1. Band diagrams of an all-silicon homojunction transistor and a $\text{Si}/\text{Si}_{1-x}\text{Ge}_x/\text{Si}$ narrow bandgap base HBT illustrating the reduced electron barrier in the HBT.

While the above principle has long been known, its implementation requires that a high-quality, low-defect heterojunction be formed on silicon. This had been hampered by the lack of a suitable semiconductor lattice-matched to silicon. $\text{Si}_{1-x}\text{Ge}_x$ alloys have a lattice constant larger than that of silicon because of the larger size of the Ge atom. However, thin $\text{Si}_{1-x}\text{Ge}_x$ layers can be grown lattice-matched to silicon by growing them in a state of compressive strain. In this state the lateral lattice constant matches that of silicon, while the vertical one is much larger [1]. These strained layers are advantageous not only because the strain eliminates defects such as misfit dislocations at the $\text{Si}/\text{Si}_{1-x}\text{Ge}_x$ interface, but also because the strain splits the usual degeneracies of the band edges. This causes the bandgap of the strained $\text{Si}_{1-x}\text{Ge}_x$ alloys to be reduced even further from that of silicon than would be expected from the presence of the Ge alone [2]. For example, an unstrained $\text{Si}_{0.8}\text{Ge}_{0.2}$ layer (which would have an enormous number of defects at a silicon interface) would have a bandgap ~ 90 meV less than that of silicon. A strained $\text{Si}_{0.8}\text{Ge}_{0.2}$ layer would have a bandgap reduction (ΔE_G) of ~ 170 meV compared to silicon, however.

In the $\text{Si}/\text{strained } \text{Si}_{1-x}\text{Ge}_x$ system, the bandgap offset is almost entirely in the valence band [3]. Therefore the increase in collector current for a given

Model Paper

change in bandgap for the same bias and similar doping can be approximated as $\frac{I_{C,SiGe}}{I_{C,Si}} = \exp\left(\frac{\Delta E_G}{kT}\right)$ [4]. For a composition of $Si_{0.8}Ge_{0.2}$, this exponential increase in emitter efficiency at room temperature is approximately a factor of ~ 500 . Achieving such improvement requires careful consideration of the location of the heterojunction with respect to the doping junction, however [5].

Device and Circuit Results

Discrete Devices

Room temperature Gummel plots of I_C and I_B vs. V_{BE} for HBT's with varying amounts of Ge in the base (and hence different bandgaps) are shown in Fig. 2 and Fig. 3 [6]. As the Ge content in the base is raised, the collector current increases monotonically as expected. Also important is that the base current does not change as Ge is added to the base, as expected from the band diagram in Fig. 1. Such base current results require high lifetimes in the $Si_{1-x}Ge_x$ layers, and to date have been obtained by Rapid Thermal

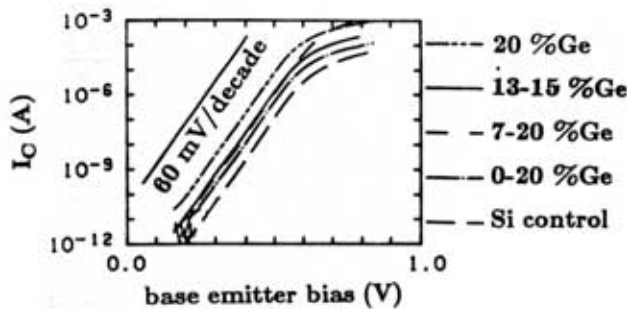


Fig. 2. Collector current vs. V_{BE} for an all-silicon control device and HBT's with varying amounts of Ge in the base (0-20% graded, 7-20% graded, 13-15% graded, and 20% flat).

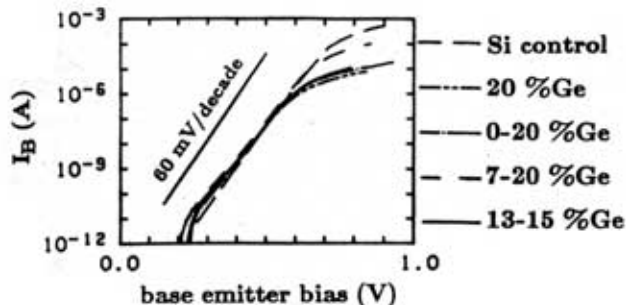


Fig. 3. Base current vs. V_{BE} for the devices of Fig. 2.

Chemical Vapor Deposition (Fig. 3) [6], UHV-CVD [7], and by MBE [8]. The design advantage of the HBT's is also demonstrated in Fig. 4, which compares the common-emitter characteristics of an all-silicon device and a simultaneously fabricated $Si/Si_{0.86}Ge_{0.14}/Si$ device with similar doping profiles. The base resistances of the two devices are similar ($\sim 3.4 \text{ k}\Omega/\square$), but the gain of the HBT is much larger than that of the Si device (160 vs. 6).

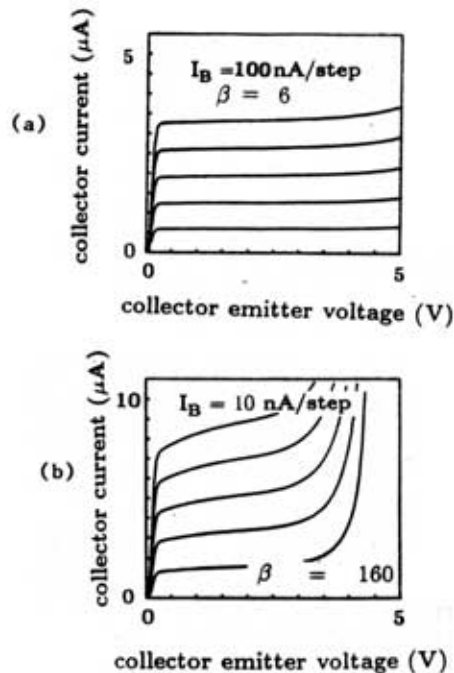


Fig. 4. Common emitter characteristics of (a) an all-silicon device and (b) a $Si/Si_{0.86}Ge_{0.14}/Si$ device with similar base resistances illustrating the higher emitter efficiency and current gain in the HBT.

Besides the emitter efficiency/base resistance advantage, a second advantage of SiGe HBT's is that the bandgap in the base can be graded by grading the Ge content across the base. This provides a built-in field which improves the base transit time. Using such an approach, Patton et al. at IBM have achieved current gain cutoff frequencies (f_t) of 75 GHz, roughly 50% higher than the best homojunction transistors fabricated by conventional ion-implanted base technology [9].

Digital Circuits

The impact of the SiGe HBT's on digital circuits such as ECL can be examined by performing SPICE simulations using a baseline of a state-of-the-art conventional process (gate delay = 27 ps). The main device parameters that will be affected are the current gain, base resistance, and cutoff frequency. For gains

over 100 (roughly the minimum required for circuit noise margin and fanout considerations), little impact of the gain on circuit delay was found. Increasing the cutoff frequency above the baseline of 27 GHz without decreasing the base resistance from its initial value of $11 \text{ k}\Omega/\square$ also had little effect (Fig. 5). The most significant parameter was the intrinsic base resistance, illustrating the importance of the HBT. By incorporating a device with an R_{Bi} of only 500Ω and not changing the cutoff frequency of 27 GHz, a $\sim 50\%$ reduction in gate delay from 27 to 14 ps should be possible. Initial circuit experiments have shown only a 15% improvement in gate delay [10], but in these devices the base resistance was still rather large ($8 \text{ k}\Omega/\square$).

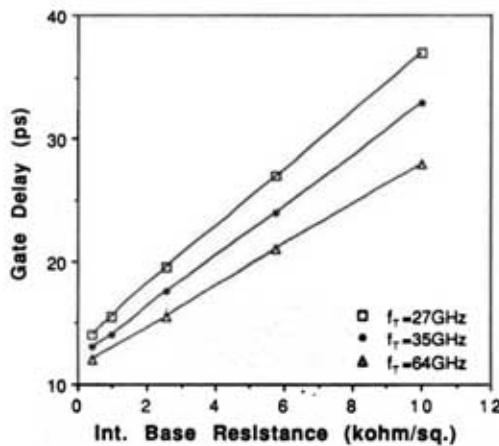


Fig. 5. Circuit simulations of ECL gate delay for various HBT designs.

Ultimate digital applications will require three integration issues to be addressed, however. These are a manufacturable approach to self alignment of epitaxial base devices, a low extrinsic base resistance so that one can benefit from low intrinsic base resistances, and a reduced thermal budget (modified poly-emitter processes, etc.) to prevent base dopant outdiffusion and the resulting parasitic barrier formation [5], and strain relaxation in the SiGe layer.

Analog Applications

The most significant impact of HBT's could be in the area of high speed and high precision analog circuitry such as D/A converters and op-amps. The performance of such circuits depends critically on the product of current gain (β) and Early voltage (V_A). Physically, a non-infinite V_A results from the fact that a reverse-biased collector-base junction decreases the width of the base and thus reduces the width of the potential barrier for electrons. This leads to a higher flow of electrons over the barrier (I_C), and hence an undesirable dependence of I_C on the collector voltage.

This effect can be suppressed in a Si/SiGe/Si HBT by putting a low bandgap region on the collector side of the base (Fig. 6) [11]. Since the collector current is controlled mostly by the high barrier (near the emitter in this device), and the collector voltage will only modulate the width of the low barrier near the collector, this device will have a very high Early voltage. Conversely, placing the low barrier (low bandgap) region on the emitter side of the base and the high barrier on the collector side of the device, a very low Early voltage should result (Fig. 7). Since the maximum barrier in the two devices is the same, experimental results of the two devices show similar gain (1400-1800), but the Early voltage of the properly designed device is ~ 20 times larger (120 vs. 6V) (Fig's. 8,9). The resulting $\beta \cdot V_A$ product of the device of Fig's 6 and 8 of $> 160,000 \text{ V}$ represents an increase of over two orders of magnitude increase in this figure of merit compared to conventional devices with similar frequency performance (Fig. 10) [12]. Furthermore, since this improvement can be achieved with only very thin low bandgap $\text{Si}_{1-x}\text{Ge}_x$ layers (high x) near the collector junction, the critical thickness concerns are significantly relaxed compared to those in devices requiring a low bandgap throughout the entire base.

Summary

$\text{Si}_{1-x}\text{Ge}_x$ strained alloys offer an attractive heterojunction solution to the emitter efficiency/base resistance trade-off in silicon-based bipolar transistors. A factor of two reduction in ECL gate delay should be possible, although process integration will be an important issue. In contrast with the possible factor of two improvements in digital gate delay and $\sim 50\%$ improvements in cutoff frequency, the largest impact of Si/Si $_{1-x}$ Ge $_x$ Si HBT's may be in the area of high performance analog applications, where an increase of more than two orders of magnitude in the $\beta \cdot V_A$ products has been demonstrated.

The support and interest of Dr. A. Goodman of ONR and of NSF is gratefully appreciated. One of the authors (E.J. Prinz) was also partially supported by IBM.

References

1. J.C. Bean, L.C. Feldman, A.T. Fiory, S. Nakahara and I.K. Robinson, *J. Vac. Sci. Technol.* **A2**, 436 (1984).
2. R. People, *Phys. Rev.* **B32**, 1405 (1985).
3. C.G. Van de Walle and R.M. Martin, *Phys. Rev.* **B34**, 5621 (1986).
4. C.A. King, J.L. Hoyt, and J.F. Gibbons, *IEEE Trans. Electron Devices*, **36**, 2093 (1989).

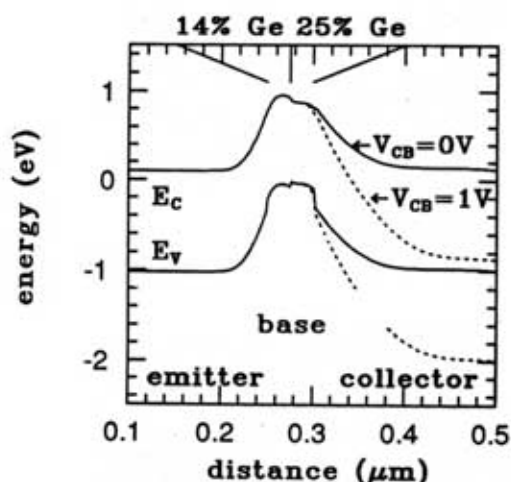


Fig. 6. Band diagram of a HBT with a smaller base bandgap ($\text{Si}_{0.75}\text{Ge}_{0.25}$) close to the collector than close to the emitter ($\text{Si}_{0.86}\text{Ge}_{0.14}$), under zero and reverse collector bias.

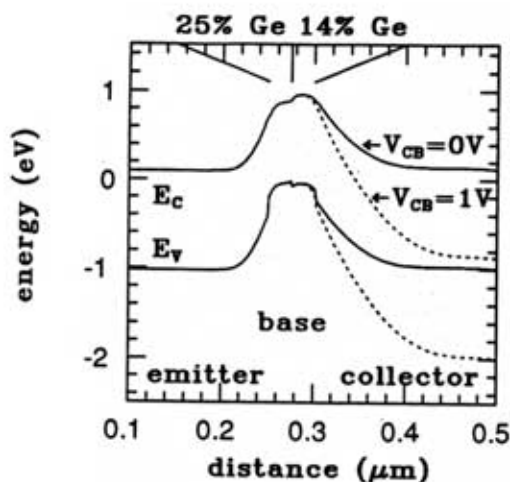


Fig. 7. Band diagram of a HBT with a larger base bandgap ($\text{Si}_{0.86}\text{Ge}_{0.14}$) close to the collector than close to the emitter ($\text{Si}_{0.75}\text{Ge}_{0.25}$), under zero and reverse collector bias.

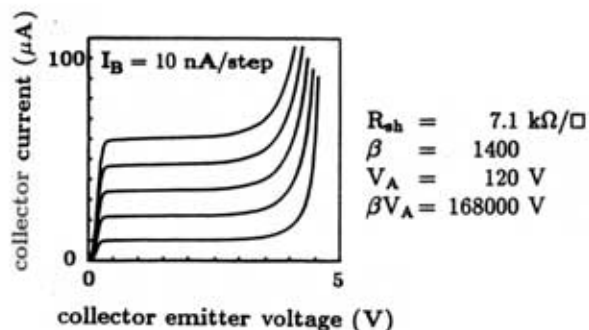


Fig. 8. Common emitter characteristics of the device of Fig. 6.

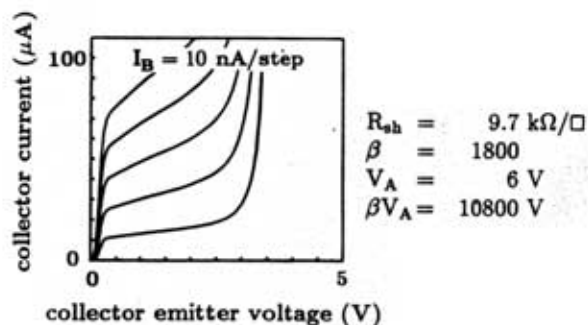


Fig. 9. Common emitter characteristics of the device of Fig. 7.

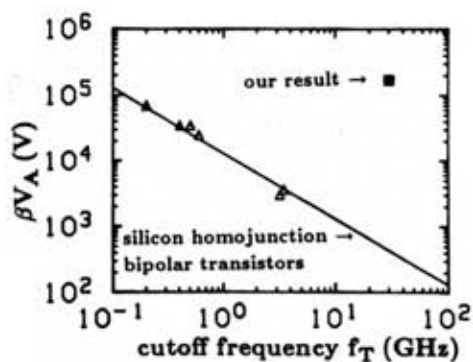


Fig. 10. Comparison of βV_A data for the HBT structure of Figs. 6, 8 compared to conventional silicon transistors.

5. E.J. Prinz, P.M. Garone, P.V. Schwartz, X. Xiao, and J.C. Sturm, *IEEE Electron Dev. Lett.*, **EDL-12**, 42 (1991).
6. J.C. Sturm and E.J. Prinz, *IEEE Electron Dev. Lett.* **EDL-12**, 303 (1991).
7. G.L. Patton et al., *IEEE Electron Dev. Lett.*, **EDL-10**, 534 (1989).
8. A. Pruijboom, et al., *IEEE Electron Dev. Lett.* **EDL-12**, 357 (1991).
9. G.L. Patton et al., *IEEE Electron Dev. Lett.* **EDL-11**, 171 (1990).
10. J.H. Comfort et al., 1990 IEDM Technical Digest, 21.
11. E.J. Prinz and J.C. Sturm, presented at the 1991 Device Research Conf., Boulder, CO, June, 1991.
12. Private communication, J. Lapham, Analog Devices.